Towards a unified approach for modelling uniform and non-uniform bubbly flows

Ziegenhein, T.; Rzehak, R.; Ma, T.; Lucas, D.;

Originally published:

September 2016

Canadian Journal of Chemical Engeneering 95(2017)1, 170-179

DOI: https://doi.org/10.1002/cjce.22647

Perma-Link to Publication Repository of HZDR:

https://www.hzdr.de/publications/Publ-22601

A unified approach for modeling uniform and non-uniform bubbly flows

T.Ziegenhein, R.Rzehak, T.Ma, D.Lucas

Abstract: An important ingredient of closure relations for the Euler-Euler two-fluid model is the description of turbulent fluctuations. Models proposed in the literature disagree concerning the treatment of such on all scales. The large scale fluctuation structures as well as the bubble induced turbulence might be neglected or resolved and/or modeled respectively in different ways. Each treatment has been demonstrated to work for a certain application but a unifying perspective is lacking so far.

To this end a set of closure relations for the fluid dynamics of bubbly flow has been collected that represents the best available knowledge and may serve as a baseline for further improvements and extensions. This model comprises a set of bubble forces as well as a turbulence model including turbulence modification due to the bubbles and has been successfully validated for bubbly flows in pipes and bubble columns. Here it is applied to two sets of data representing non-uniform and uniform flows in bubble columns which are dominated by large scale fluctuations and bubble induced turbulence respectively.

Keywords: dispersed gas-liquid multiphase flow, Euler-Euler two-fluid model, CFD simulation, bubble column, bubble-induced turbulence

INTRODUCTION

Bubble columns are widely used in industrial applications since they enable an effective mass transfer between the gaseous and liquid phase. The performance of a bubble column strongly depends on the characteristics of the flow. Basically, two flow regimes with different characteristics exist in bubble columns. In one of them there is a more or less uniform flow pattern with a uniform distribution of the gas content over the cross section. The other flow regime is characterized by large scale flow structures with a non-uniform flow pattern which arise from unevenly distributed gas content and/or as a consequence of bubble coalescence and break-up processes. [1] Therefore, the bubble sizes in this regime are often ranging from very small to very large bubbles. The uniform flow regime in contrast has a rather narrow bubble size distribution due to the absence of coalescence and breakup. In this context they are also referred as heterogeneous and homogeneous regimes, respectively. Because of the different flow patterns the dominant turbulent structures in heterogeneous and homogenous regimes might be different.

Modeling the turbulence in bubbly flows is essential since many other processes such as coalescence and breakup (e.g. Liao et al. [2]) or mass transfer (e. g. Wang & Wang [3]) are influenced by the presence of turbulence structures. A great effort has been made over the last years to describe the interaction of the bubbles with turbulent structures and the turbulence produced by bubbles itself. Discussions about this topic are given for example by Risso et al. [4] or Riboux et al. [5]

In practice, two approaches for modeling turbulence in bubbly flows are mostly used for CFD simulation. The first assumes a superposition of the contributions to the turbulent viscosity due to shear- and bubble-induced turbulence. [6] [7] The shear-induced contribution is determined using a two-equation turbulence model like the k-ϵ model [8] for single phase flow while for the bubble-induced contribution a correlation is given by Sato et al. [6] This approach gives good results regarding gas fraction and liquid velocity profiles both in pipe flows [9] and in bubble columns [10]. The turbulent kinetic energy, however, is underpredicted in both configurations. [11] [12] The second frequently used approach assumes a superposition of the production terms for shear- and bubble-induced turbulence. Hence, both production terms are added in the two equation turbulence model and the turbulent viscosity is then calculated by the usual relation. This approach provides

reasonable estimates, particularly for the turbulent kinetic energy in both pipes [13] and bubble columns [14].

Both approaches discussed so far are based on two-equation RANS-modeling. Other approaches for turbulence modeling in general have been applied to bubbly flows as well. For bubble columns in particular simulations using Reynolds stress models (RSM) [15] and large eddy simulations (LES) [16] have been used. However, the bubble induced turbulence is typically neglected in these approaches like in earlier unsteady RANS simulations. [17]

An experimental setup for non-uniform flows that is frequently used to validate simulation models is that of partially aerated bubble columns. Examples are the works of Becker et al., [18] Pfleger et al. [19], or Deen et al. [20] The outcome of such studies is often that the hydrodynamics could be well predicted even by neglecting the bubble induced turbulence [21] or bubble forces like the lift force [22]. More recently, Ojima et al. [23] concluded that even without any turbulence modeling non-uniform bubbly flows with large vortex structures could be well described.

The intent of the present work is to show that by modeling the bubble induced turbulence using source terms combined with the consideration of all reasonable bubble forces both regimes, non-uniform bubbly flows with large vortex structures and uniform bubbly flows, can be reproduced by a single model. For this purpose, the unsteady RANS equations combined with the baseline model for bubbly flows proposed by Rzehak & Krepper [24] are used as suggested by Ziegenhein et al. [12]. An approach that is capable to model both regimes is essential for reliable CFD calculations since geometrical changes of the facilities can lead to a regime transition as well as bubble coalescence and breakup. [25] For the present investigation the non-uniform regime is represented by a partially aerated bubble column so that a fixed bubble size distribution can be imposed which bypasses the additional complexity and uncertainty of modeling bubble coalescence and breakup. For this purpose the experimental data of Deen et al. [20] are used. The homogenous regime is investigated using the experimental data of Julia et al. [26] with a uniform gas injection.

PHYSICAL MODELING

In the present work the Eulerian two-fluid model is used. This approach has been discussed in a number of books (e.g. Ishii & Hibiki [27]), while its application to bubble columns is covered in

several reviews (e.g. Jakobsen, et al. [28]). In the two-fluid model the multiphase problem is described through averaged equations. As a result the interaction between the dispersed gas phase and the continuous liquid phase has to be modeled. This concerns forces acting on the liquid and dispersed phases and the induced turbulence in the liquid because of the motion of the dispersed phase. Development and validation of such closure models is an active area of research. In the present work a set of models is used which has recently been applied with good success by Rzehak & Krepper, [24] [29] Rzehak & Kriebitzsch, [30] Rzehak et al. [31] and Ziegenhein et al. [12] [32].

Further, in the present work the URANS approach is used as suggested by Ziegenhein et al. [12]. In principle, with the URANS approach the turbulent fluctuations consist of two parts. The resolved part contains the unsteady large-scale flow structures which are obtained directly from the time-dependent liquid velocity field. The unresolved part contains all small-scale motions including the bubble induced turbulence (BIT). In this paper the BIT is modeled with source terms in the two-equation model of the URANS approach. The extra source of turbulent kinetic energy from the bubbles is usually modeled as the power due to the relative motion between the bubbles and the liquid. A lack of agreement exists regarding the source term for the turbulent dissipation rate. Different approaches were proposed over the last years, e.g. by Morel, [33] Troshko & Hassan [34] or Politano et al. [35] Recently Rzehak and Krepper [13] performed a detailed study of different BIT models and formulated an own model which turned out to be the most reliable model for their test cases. In addition, this model gives also the best results in a bubble column test case studied by Ziegenhein et al. [14].

URANS

URANS calculations are based on the traditional RANS approach but retain the time-dependence in the equations of motion. The relatively simple and fast URANS calculations are used in a wide range of application, for example they are capable to reproduce the vortex shedding at bluff bodies as discussed by Spalart. [36]. With the URANS approach the fluctuations of the velocity are decomposed in resolved and unresolved parts. For comparison with experiments both parts have to be considered, thus the total normal components of the Reynolds stress tensor are calculated by summation of the resolved part $\overline{\widetilde{v'}\widetilde{v'}}$ and the unresolved part $2/3\,\overline{k_{mod}}$

$$\overline{v'v'} = \overline{\widetilde{v'}\widetilde{v'}} + \frac{2}{3}\overline{k_{mod}}\,. \tag{1}$$

The same is done for the horizontal velocity u. With k_{mod} the modeled turbulence kinetic energy from the two equation model which is denoted further on simply as k.

Bubble Induced Turbulence

For the continuous phase, the shear-induced turbulence is described by the SST model with parameters taking their usual single phase values. The BIT is included by additional source terms. The turbulence of the dispersed phase is assumed to be negligible since the density is very small compared to the continuous phase. Therefore, it is not explicitly modeled.

Concerning the source term describing bubble effects in the k-equation, a plausible approximation is provided by the assumption that all energy lost by the bubble due to drag is converted to turbulence kinetic energy in the wake of the bubble. Hence, the k-source becomes

$$\mathrm{S_L^k} = \mathrm{F_{Drag}}|\vec{v}_G - \vec{v}_L|\,. \tag{2}$$

For the ϵ -source a similar heuristic is used as for the single phase model, namely the k-source is divided by some time scale τ so that

$$\mathrm{S_L^\epsilon} = \frac{\mathrm{C_{\epsilon B}}\left(\mathrm{S_L^k}\right)}{\tau}\,. \tag{3}$$

Modeling of the time scale τ proceeds largely based on dimensional analysis. There are two velocity and two length scales for this problem, in which one of each is related to the bubble and the other to the turbulent eddies, thus four plausible time scales can be formed. All four time scales were compared by Rzehak and Krepper [13] and Ziegenhein et al. [14] and it was found that the best predictions were obtained for

$$\tau = \frac{d_B}{\sqrt{k_L}} \tag{4}$$

together with a value of $C_{\epsilon B} = 1.0$.

For the use with the SST model, the ϵ -source is transformed to an equivalent ω -source which gives

$$S_L^{\omega} = \frac{1}{C_{\mu} k_L} \, \mathrm{S}_{\mathrm{L}}^{\epsilon} - \frac{\omega_L}{k_L} \, \mathrm{S}_{\mathrm{L}}^{\mathrm{k}} \, . \tag{5}$$

The ω -source is used independently of the blending function in the SST model since it should be effective throughout the fluid domain.

Finally, the eddy viscosity is evaluated from the standard formula

$$\mu_L^{turb} = C_{\mu} \rho_L \frac{k_L^2}{\epsilon_L} . \tag{6}$$

Bubble Forces

Drag force

The drag force is a momentum exchange because of a slip velocity between the gas and the liquid. This is modeled with a sink in the gas momentum equation

$$F_{Drag} = \frac{3}{4 d_B} C_D \rho_L \alpha_G |\vec{v}_G - \vec{v}_L| (\vec{v}_G - \vec{v}_L) \, . \tag{7}$$

The drag coefficient C_D for the bubble regime investigated here depends on the Reynolds number and the Eötvös number. A correlation distinguishing different shape regimes has been suggested by Ishii and Zuber [37] namely

$$C_D = \max\left(C_{D,sphere}, C_{D,ellipse}\right) , \tag{8}$$

where

$$C_{D,sphere} = \frac{24}{Re} (1 + 0.1 Re^{0,75}) , \tag{9}$$

$$C_{D,ellipse} = \frac{2}{3} Eo^{0.5} \, . \tag{10}$$

Tomiyama et al. [38] validated this correlation and found good agreement except at high values of the Eötvös number.

Lift force

In a shear flow a bubble experiences a force lateral to the direction of flow. This is commonly referred to as the lift force and described by the definition of Zun [39]

$$F_{Lift} = -C_L \rho_L \alpha_G (\vec{v}_G - \vec{v}_L) \times rot(\vec{v}_L)\,. \tag{11}$$

For a spherical bubble the shear lift coefficient C_L is positive so that the lift force acts in the direction of decreasing liquid velocity, i.e. in case of co-current pipe flow in the direction towards the pipe wall. Experimental (e.g. [40]) and numerical (e.g. [41]) investigations showed that the direction of the lift force changes its sign if a substantial deformation of the bubble occurs. From the observation of the trajectories of single air bubbles rising in simple shear flow of a glycerol water solution the following correlation for the lift coefficient was derived

$$C_L = \begin{cases} \min[0.288\tanh(0.121\,Re), f(Eo_\perp)] & Eo_\perp < 4 \\ f(Eo_\perp) & 4 \le Eo_\perp < 10 \\ -0.27 & Eo_\perp \ge 10 \end{cases}, \tag{12}$$

with

$$f(Eo_\perp) = 0.00105Eo_\perp^3 - 0.0159Eo_\perp^2 - 0.0204Eo_\perp + 0.474\,. \tag{13}$$

Here the modified Eötvös number is given by

$$Eo_\perp = \frac{g(\rho_L - \rho_G)d_\perp}{\sigma}, \tag{14}$$

where σ is the surface tension and $d_\perp$ is the maximum horizontal dimension of the bubble. It is calculated using an empirical correlation for the aspect ratio by Wellek et al. [42]

$$d_\perp = d_B \sqrt[3]{1 + 0.163Eo^{0.757}}\,, \tag{15}$$

where Eo is the usual Eötvös number. The usual Eötvös number Eo is calculated with the bubble diameter d_B as the characteristic length, whereas the modified Eötvös number $Eo_\perp$ is calculated with the maximum horizontal dimension of the bubble as the characteristic length.

The experimental conditions on which Equation (12) is based were limited to the range $-5.5 \le \log_{10} Mo \le -2.8, 1.39 \le Eo \le 5.74$ and values of the Reynolds number based on bubble diameter and shear rate $0 \le Re \le 10$. The water–air system at normal conditions has a Morton number $Mo = 2.63 \times 10^{-11}$ which is quite different. Nevertheless, for this case the diameter where the lift force changes its direction could be shown by Lucas and Tomiyama [43] to be in good agreement with the model. As can be seen from Eqs. (12) and (13) this diameter is about 5.8 mm.

Wall force

A bubble translating next to a wall in an otherwise quiescent liquid also experiences a lift force. This wall lift force, often simply referred to as wall force, has the general form

$$F_{Wall} = \frac{2}{d_B} C_W \rho_L \alpha_G |\vec{v}_G - \vec{v}_L|^2 \, \hat{y} \,, \tag{16}$$

where $\hat{y}$ is the unit normal perpendicular to the wall pointing into the fluid. The dimensionless wall force coefficient C_W depends on the distance to the wall y and is expected to be positive so the bubble is driven away from the wall. Based on the observation of single bubble trajectories in simple shear flow of glycerol water solutions Tomiyama et al. [44] and later Hosokawa et al. [45] concluded the functional dependence

$$C_W(y) = f(Eo) \left(\frac{d_B}{2y}\right)^2 , \tag{17}$$

where in the limit of small Morton number [45]

$$f(Eo) = 0.0217 Eo \,. \tag{18}$$

The experimental conditions on which Equation (18) is based are $2.2 \leq Eo \leq 22$ and $-2.5 \leq \log_{10} Mo \leq -6.0$ which is still different from the water–air system with $Mo = 2.63 \times 10^{-11}$. A recent comparison of this and other distance-dependencies that have been proposed [46] has nonetheless shown that good predictions could be obtained for a set of data on vertical pipe flow of air bubbles in water.

Turbulent dispersion force

The turbulent dispersion force describes the effect of the turbulent fluctuations of the liquid velocity on the bubbles. In Burns et al. [47] an explicit expression is derived by Favre averaging the drag force, namely

$$F_{Disp} = \frac{3}{4} C_D \frac{\alpha_G}{d_B} |\vec{v}_G - \vec{v}_L| \frac{\mu_L^{turb}}{\sigma_{TD}} \left(\frac{1}{\alpha_L} + \frac{1}{\alpha_G}\right) \nabla \alpha_G \,. \tag{19}$$

In analogy to molecular diffusion σ_{TD} is referred to as a Schmidt number. In principle it should be possible to obtain its value from single bubble experiments by evaluating the statistics of bubble trajectories in well-characterized turbulent flows but to the authors knowledge this has not been done yet. A value of $\sigma_{TD} = 0.9$ is typically used.

Virtual mass

The virtual mass is the inertia of the surrounding fluid that has to be taken into account when a bubble or particle is accelerated relative to the surrounding continuous phase:

$$F_{VM} = C_{VM}\alpha_G\rho_G\left(\frac{D\vec{v}_G}{Dt} - \frac{D\vec{v}_L}{Dt}\right), \tag{20}$$

where D/Dt denotes the substantial derivative. The coefficient C_{VM} is simply set to 0.5 as suggested by Mougin and Magnaudet [48].

SIMULATION SETUP

As discussed above, the scope of this work is to investigate two different regimes of bubble driven flows: first, a non-uniform regime dominated by large vorticities and, second, a uniform regime without such large fluid structures. The non-uniform regime here occurs due to partial aeration of the column, while for the uniform regime gas is injected over the full column cross-section. The non-uniform regime has been investigated experimentally by Deen et al. [20] and the uniform regime by Julia et al. [26]. A sketch of both experimental setups is shown in Figure 1. The gas volume flow rates and bubble sizes are summarized in Table 1.

The bubble column used by Deen et al. [20] has a quadratic ground plate and an initial water level of 0.45 m. The sparger consist of an array of 7 by 7 holes. Air and water are used as materials with 0.04 weight % of kitchen salt are added to suppress coalescence. Mean and fluctuations of liquid velocities are measured using LDA and PIV on a line 0.25 m above the ground plate. The bubble sizes are estimated as 4 mm by not further specified visual observations.

The bubble column used by Julia et al. [26] is a flat bubble column with a needle sparger consisting of 137 uniformly distributed needles. Air and water are used as materials. Mean and fluctuations of liquid velocities are measured with LDA on a line 0.6 m above the ground plate. The bubble sizes have been obtained by single needle experiments using video cameras.

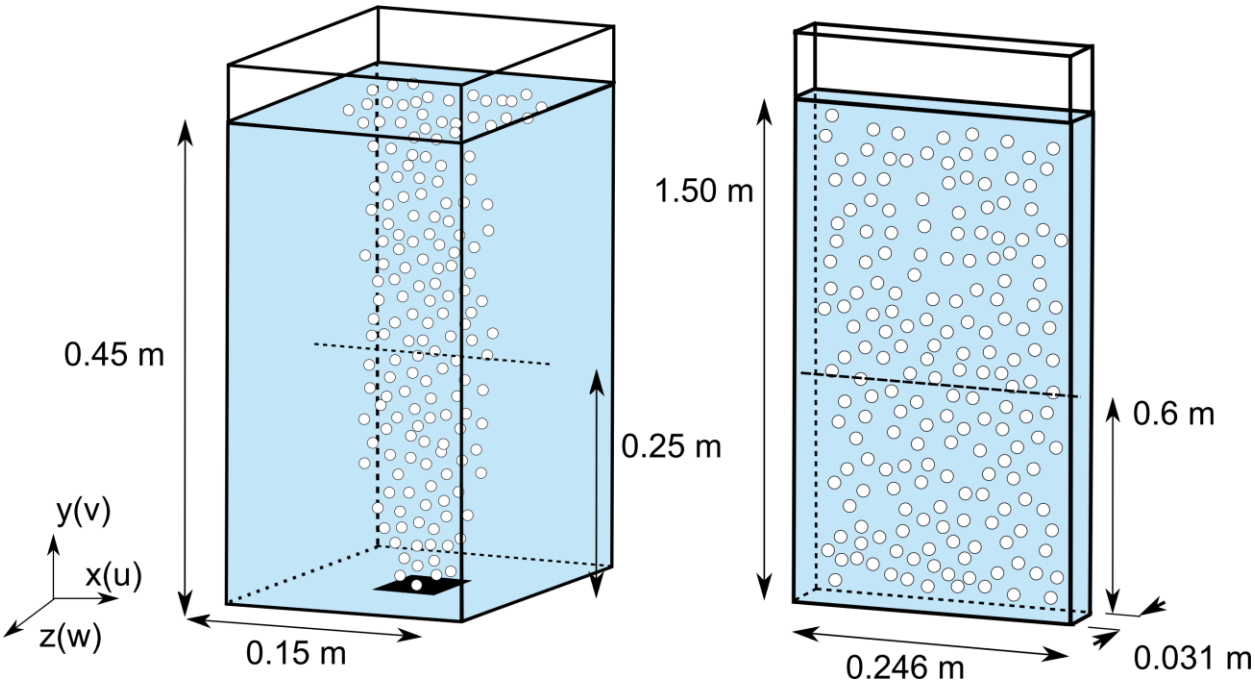

Figure 1 Sketch of the experimental setups. Left: The setup of Julia et al. [26]. Right: the setup of Deen et al. [20]. The measurement positions are shown as dotted lines.

Author	Superficial velocity [mm/s]	Bubble size [mm]
Deen et al. [20]	4.9	4
Julia et al. [26]	21	3.66
	29	3.82
	43	4.09
	58	5.6

Table 1 The superficial gas velocities and bubbles sizes used in the experiments and CFD simulations.

For both cases grid studies were conducted. As a result, the bubble column of Deen et al. [20] is discretized using a uniform cubic mesh of 5 mm cell size consisting of 81 000 cells. The bubble column of Julia et al. [26] is, likewise, discretized using a uniform rectangular mesh of $\Delta x = 5\text{mm},\ \Delta y = 8.2\text{ mm},\ \Delta z = 5.1\bar{6}$ size, consisting of 90 000 cells.

On the walls a no slip condition is imposed for the continuous phase and a slip condition for the dispersed phase. The top of the column is treated as a degassing boundary, which means a no penetration and no slip condition for the continuous phase and an outlet condition for the dispersed phase. Here the pressure remains variable over the top of the column, which might be interpreted as different surface heights at different positions due to the flow, [49] for other scalar quantities of the dispersed phase a constant gradient is imposed. For the Deen column the inlet is modeled as a region of size of 0.03 x 0.03 m in the center of the column bottom as in the original work (Deen et al 2001). For the Julia column the inlet corresponds with the full column bottom. The gas volume flux through the inlet area is set equal to the experimental value of the superficial velocity. For the spatial discretization a high resolution scheme is used. [49] For the temporal discretization a second-order backward Euler scheme is used. The time step was set such that the Courant-Friedrich-Levi (CFL) number is below one as suggested by Ziegenhein et al. [12]. The simulations were run until reaching the convergence criteria suggested by Ziegenhein et al. [12].

RESULTS

Non-Uniform Bubbly Flow

The flow in the bubble column of Deen et al. [20] is characterized by large scale flow structures. The liquid velocities were measured using particle image velocimetry (PIV) and laser Doppler anemometry (LDA). In the following the PIV results are plotted with the LDA results as error bars to indicate the uncertainty of the experimental data.

The measurement technique to determine the bubble size is not described by Deen et al., so the reported value may not be reliable. Therefore three different bubble sizes 3, 4, and 5 mm were tested. The results are shown in Figure 2. The vertical liquid velocity varies strongly

with the bubble size, the simulation with 4 mm gives here the best results compared to experiments. In contrast, the root mean square of the normal Reynolds stress tensor components v′v′ and $u'u'$ (RMS(v′v′) and RMS(u′u′)), respectively are not as much influenced by the bubble size as the vertical liquid velocity. It should be noted however, that the RMS(v′v′) and RMS(u′u′) results shown in Figure 2 are the sum of the unresolved and resolved contributions to the turbulent fluctuations, and both individual contributions do vary with the bubble size but the total amount remains nearly the same. Since the results for 4 mm bubble size are in fact closest to the experimental data this value will be used from hereon.

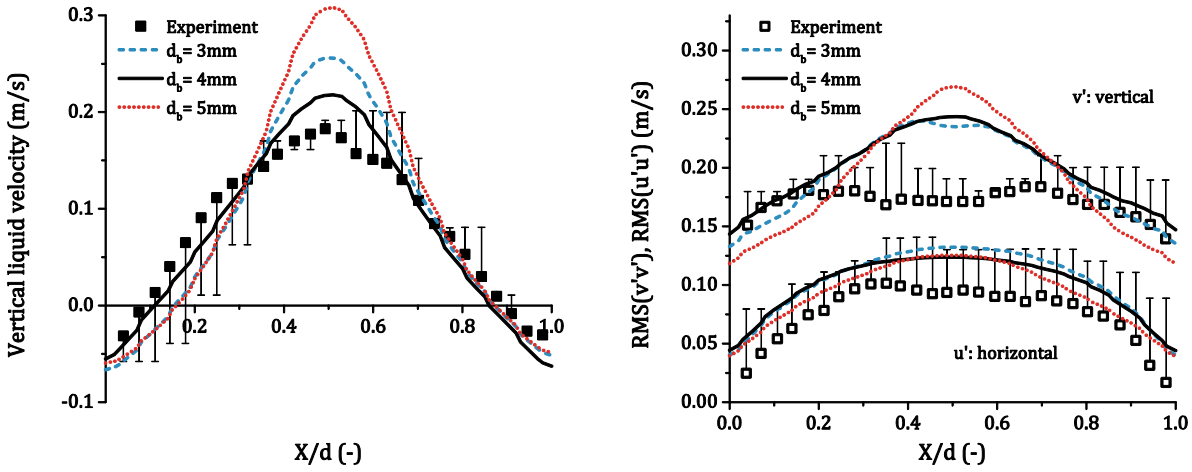

Figure 2 Simulation results using different bubble sizes compared to experiments. Left: Vertical liquid velocity. Right: Root mean square of the normal Reynolds stress tensor components $v'v'$ and $u'u'$.

The contribution of the unresolved and resolved parts of RMS(v′v′) and RMS(u′u′), obtained from the URANS modeling, are shown in Figure 3 a) and b). In addition, the results without BIT modeling are also shown for comparison in Figure 3 c) and d). For the mean liquid velocity there is no significant difference whether BIT is included or not, therefore no additional figure is shown.

Considering the measurement uncertainty, the total values of both RMS(v′v′) and RMS(u′u′) obtained by the simulations both with and without BIT are in reasonable agreement with the

data. The most prominent difference between the models with and without BIT is the shape of the total RMS(v′v′) profiles. With BIT a profile with a single center-peak is obtained with a trend to overpredict the measured values in the center of the column. Without BIT a double-peaked profile is found which is somewhat closer to the data. For both models the predicted variations are too pronounced compared with the experimental profiles which have a rather flat shape. For the total RMS(u′u′) both models give similar results.

RMS(v′v′) is dominated by the resolved contribution for both models with and without BIT. In contrast for RMS(u′u′) resolved and unresolved contributions have similar values for the model with BIT while for the model without BIT the modeled contribution is much larger than the resolved contribution.

The resolved contribution to the Reynolds stresses is higher with BIT model than without a BIT model in general. This is caused by the eight times lower eddy viscosity obtained with the BIT model. Accordingly, the eddy dissipation rate is distinctly higher with the BIT model. Nevertheless, the liquid velocity profiles (not shown) obtained with BIT und without BIT modeling are nearly the same.

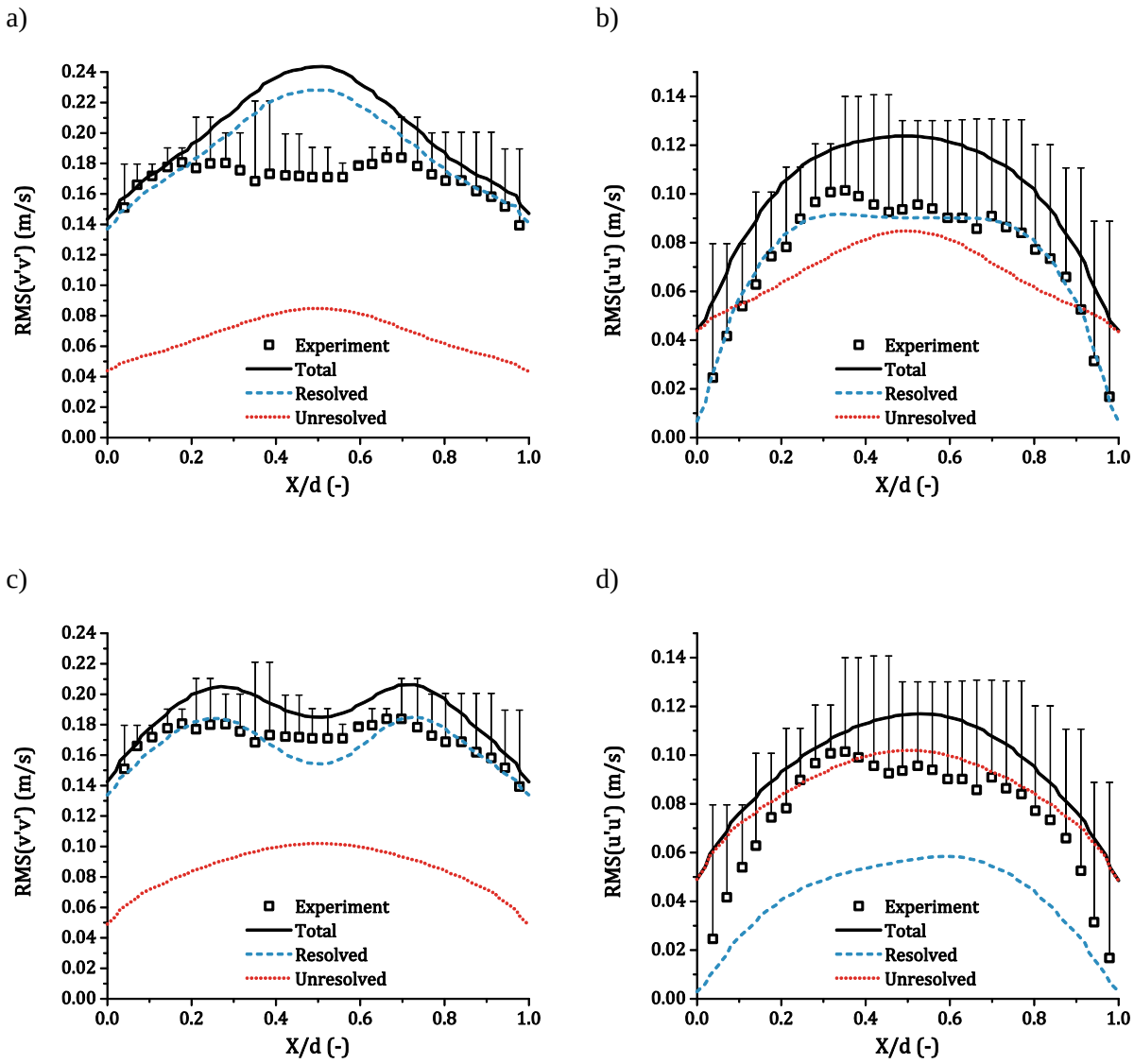

Figure 3 Resolved and unresolved parts of $RMS(v'v')$ and $RMS(u'u')$ with and without BIT at 0.25 m above sparger compared to experimental data by Deen et al. [20] a) And b) using BIT; c) and d) without a BIT model.

Summarizing, the non-uniform regime represented here by the experiments of Deen et al. [20] using a monodisperse bubble size distribution in a partially aerated bubble column can be reproduced satisfactorily using a two equation turbulence model either with or without BIT source terms. Moreover, the URANS modeling gives nearly the same results as large eddy simulations and scale adaptive simulations [16] or Reynolds stress models [15].

Uniform Bubbly Flow

The uniform regime is characterized by a uniform distribution of the bubbles over the cross section of the column. When the bubbles are small enough this situation is stabilized by the lift force as discussed by Lucas et al. [50] [25] so that no larger vorticities are expected as well as the turbulence is expected to be dominated by the BIT part. As discussed above the experiments of Julia et al. [26] are chosen for the investigation of this regime.

Profiles of the liquid velocity that were measured with LDA for the cases with gas superficial velocities of 29 mm/s and 43 mm/s are compared with the URANS modeling in Figure 4 a), b) and c), d) respectively. Simulation results obtained both with and without BIT modeling are shown. As expected, the resolved part of the fluctuations in both directions RMS(v′v′) and RMS(u′u′) turns out to be zero in the simulations for both model variants, thus only the modeled part is shown which equals the total fluctuations. As a consequence the calculated values for RMS(v′v′) and RMS(u′u′) are equal since the modeled fluctuations are isotropic.

In comparison to the non-uniform regime the liquid velocity profiles are much more plug flow like with the liquid flowing downwards only much closer to the side walls. Similarly the profiles of RMS(v′v′) and RMS(u′u′) here are almost constant over the column width and drop to zero steeply near the walls.

Comparing experiment and simulations, the vertical liquid velocity is underpredicted in the simulations for both values of the superficial velocity. As seen from the comparison of LDA and PIV data by Deen et al. (2001) (cf. Figure 3) a possible systematic error of the LDA method, which gives consistently higher values than obtained by PIV, may contribute to this deviation. From the modeling the neglect of swarm effects and the use of a drag correlation for contaminated rather than clean systems are likely to play a role. The data show characteristic peaks near the walls which are in principle also seen in the simulations but more smeared out. Simulations with and without BIT modeling give quite similar results for the vertical liquid velocity.

Concerning the fluctuations the RMS(v′v′) and RMS(u′u′) which have both been measured for the lower superficial velocity of 29 mm/s a certain anisotropy is seen which is not covered by the present two equation turbulence model. A full Reynolds stress model is

needed to capture this effect. Comparing the models with and without BIT it is seen that without a BIT model the turbulence is underpredicted by a factor of 4 or more whereas with BIT model it is overpredicted by a factor of approximately 2. The profile shape with BIT model shows peculiar peaks at the wall which are absent in the data. For the higher superficial velocity of 43 mm/s only data for RMS(v′v′) are available which show slightly higher values than for 29 mm/s. this trend is also seen in the simulations with BIT model but not in those without BIT model.

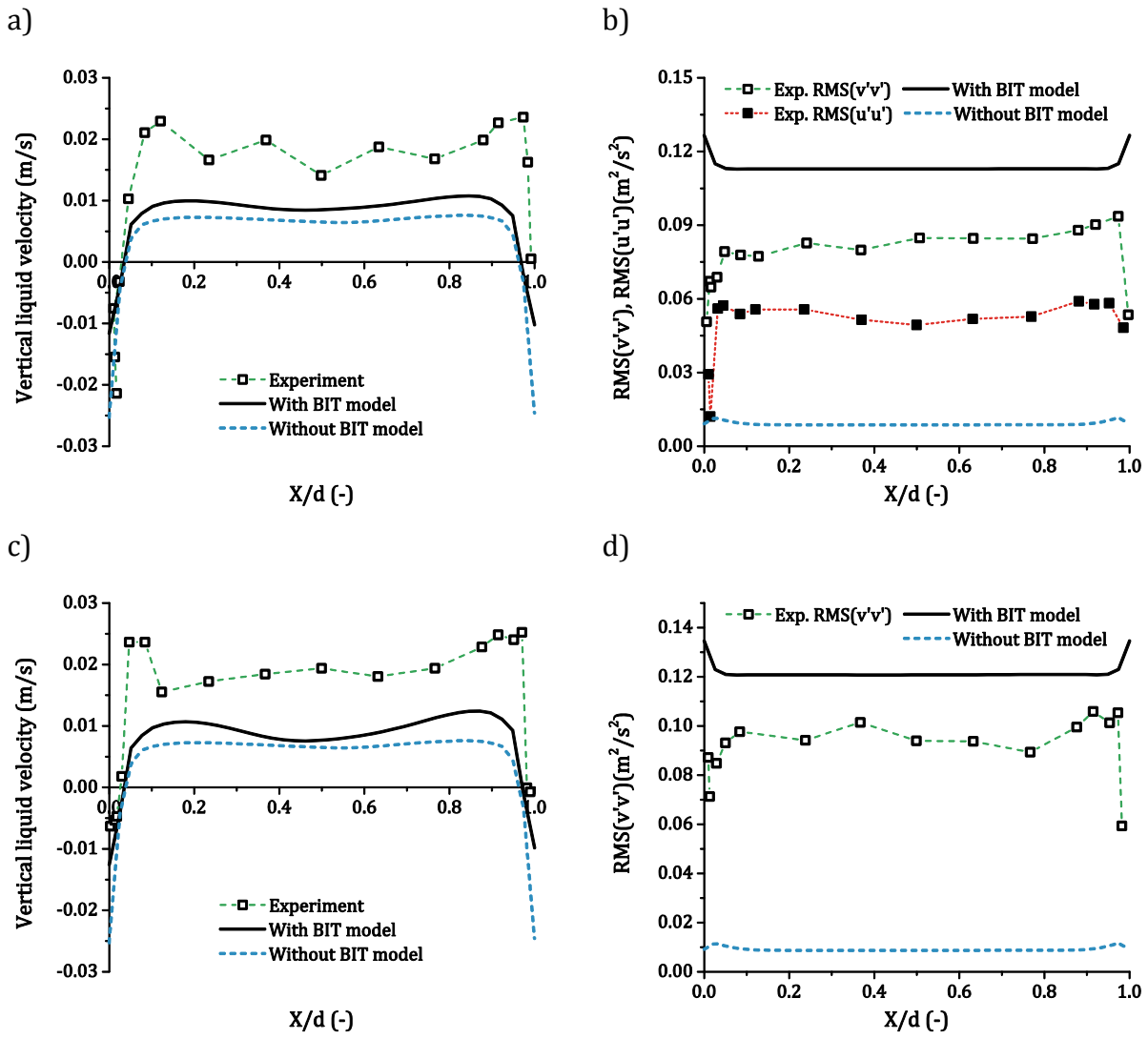

Figure 4 Vertical liquid velocity and $RMS(v'v')$ and $RMS(u'u')$ obtained with the URANS modeling compared to experiments by Julia et al. [26] *a) and b) superficial velocity of 29 mm/s. c) and d) superficial velocity of 43 mm/s.*

For all four values of superficial velocity averages of the RMS(v′v′) and RMS(u′u′) values along the measurement line have been reported by Julia et al. [26] (without the near wall region). These are shown in Figure 5 together with the corresponding simulation results for the model with BIT. As can be seen, the overprediction of the values by the simulations is present for all superficial velocities with the deviations increasing with decreasing superficial velocity.

In addition, Figure 5 shows data from another experiment for uniform flow in a bubble column by bin Mohd Akbar et al. [51] and corresponding URANS simulations from Ziegenhein et al. [12] using the same modeling as in the present study with BIT is included. The results obtained with the URANS simulations for the latter case are in good agreement with the measured RMS(v′v′).

Since the data of Julia et al. [26] and bin Mohd Akbar et al. [51] do not fall on a single curve, it appears that besides the superficial velocity some other relevant parameter must exist. The bubble sizes in both experiments are about 4 mm and both have been conducted in an air/water system. Also the geometries are rather similar the column of bin Mohd Akbar et al. [51] being about twice as thick as that of Julia et al. [26] or in other words almost twenty and ten times the bubble diameter respectively. The integral gas hold up differs strongly between the two experiments, for the experiments of bin Mohd Akbar et al. [51] is about 1.5 % while for the experiments by and Julia et al. [26] ranges from 5.4 % to 20.2 %. However this difference corresponds with the different superficial velocity. Therefore it is not clear where the mismatch between both experiments comes from.

In Julia et al. [26] it is mentioned that a turbulence model for bubbly flows based on the pseudo turbulence obtained from potential flow [52] with a dependency on the void fraction as $\alpha^{2/3}$ [53] can reproduce their experimental data. However, additional simulations performed using this model have shown heavy underprediction for the experiments by bin Mohd Akbar et al. [51] Hence, such a model adaptation is not useful in general. Moreover, introducing a similar void fraction dependence in the pre factor $C_{\epsilon B}$ of the present BIT model would also worsen the agreement for the experiments by bin Mohd Akbar et al. [51] and probably also for the pipe flow tests by Rzehak & Krepper [24] [29] and Rzehak & Kriebitzsch [30].

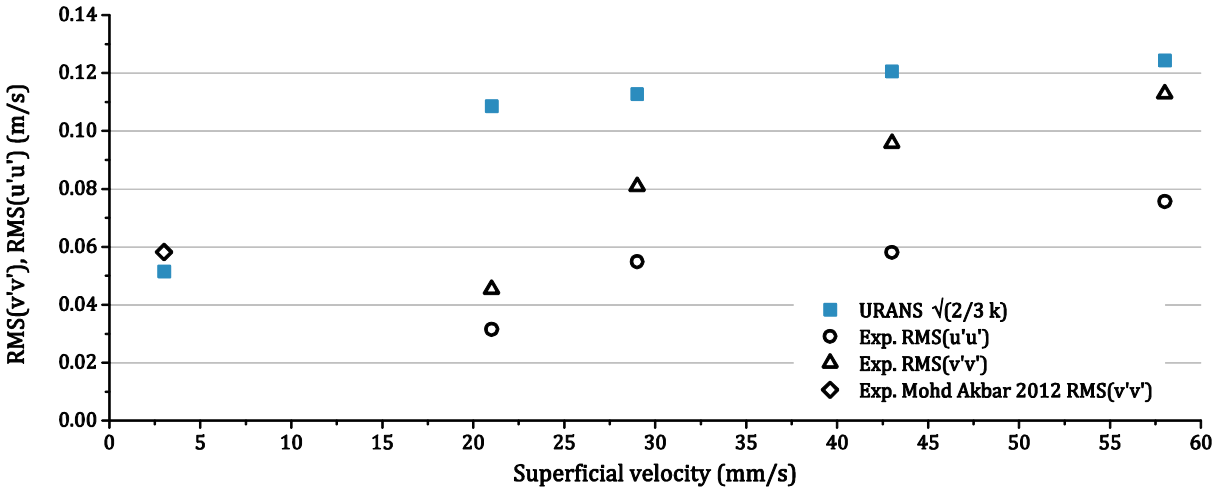

Figure 5 Reynolds stresses for uniform flow in bubble columns at different superficial velocities. The four superficial velocities from [26] with simulations from the present study and the experiments by bin Mohd Akbar et al. [51] with the corresponding URANS simulations by Ziegenhein et al. [12] are shown.

Summarizing, the uniform regime represented by the experiments of Julia et al. [26] can be roughly reproduced by the URANS approach. The resolved part of the turbulence modeling is zero as may be expected and the simulated RMS(v′v′) and RMS(u′u′) are completely dominated by the used BIT model.

Discussion

Transient simulations with a turbulence modeling based on the URANS approach were performed for a uniform and a non-uniform bubbly flow regime as represented by experiments by Deen et al. [20] and Julia et al. [26]. The bubble induced turbulence (BIT) was modeled using source terms in the two equation turbulence model. Thus, the large scale flow structures are obtained directly from the variance of the velocity field, while the small scale structures including the BIT are modeled using the two equation model. A set of closure models recommend by Rzehak & Krepper [24] with extension to URANS modeling by [12] has been used. In addition, the results obtained with the used BIT model have been compared to simulations without BIT modeling.

The non-uniform bubbly flow regime that contains larger scale flow structures is very well reproduced by the URANS approach. The resolved structures obtained from the simulations give an important contribution to the turbulence. In the sideward direction the resolved part is of the

same magnitude as the unresolved part. In contrast, in the vertical direction the resolved part is distinctly larger than the unresolved part. Compared to the results without BIT modeling the resolved turbulence is slightly smaller when using the BIT model. Further, the resolved turbulence in the sideward direction without a BIT model is distinctly smaller than with the BIT model, in the vertical direction the resolved part for both models is in the same range. However, both simulation setups, with and without BIT, can reproduce the experiments in the range of the expected uncertainty very well. Moreover, comparing the URANS results to other turbulence model approaches like LES [16] or RSM [15] no large differences can be seen.

A different situation can be found in the uniform bubbly flow regime. Here, the liquid velocity is small and no large scale flow structures are expected. The results obtained from the URANS simulations are consistent with this expectation. The liquid velocity obtained from the URANS simulations is small and the resolved turbulence part is nearly zero. Therefore, the turbulence is completely characterized by the model for the unresolved turbulence. Simulations without BIT modeling heavily underpredict the turbulence in this regime. The results obtained from the simulations with BIT in contrast overpredict the experimental data to somewhat lesser degree with deviations increasing with decreasing superficial velocity. Despite the necessity to improve the modeling further, the URANS approach with the BIT model used here is capable to describe the uniform bubbly flow regime as well.

While the modeling of the source terms representing the BIT still remains an issue of active research the results obtained here are very promising, because a single BIT model is applied without any adjustments to both non-uniform and uniform flows in bubble columns. In addition the same model has been previously applied successfully also to an intermediate situation where both large scale fluctuation structures and bubble induced turbulence are important [12] and to turbulent bubbly pipe flows [24] [29] and Rzehak & Kriebitzsch [30]. Indeed, also the present BIT model with the URANS approach is capable to reproduce nearly the exact turbulence values in uniform bubbly flows as recently shown by Ziegenhein et al. [12].

A desirable improvement of the turbulence modeling is an extension to a full Reynolds stress model including source terms for the BIT that is capable to represent anisotropic turbulent fluctuations. Moreover, the inclusion of swarm effects in all bubble forces as well as a consistent

description of clean and contaminated systems are needed. Finally the quest for more accurate measurement data is a challenging but urgent issue.

ACKNOWLEDGEMENT

This work was funded by the Helmholtz Association within the frame of the Helmholtz Energy Alliance “Energy Efficient Chemical Multiphase Processes” (HA-E-0004).

NOMENCLATURE

Notation	Denomination
$C_{\varepsilon B}$	bubble-induced turbulence coefficient
C_D	drag coefficient
C_L	lift coefficient
C_{TD}	turbulent dispersion coefficient
C_{VM}	virtual mass force coefficient
C_W	wall force coefficient
C_ε	shear-induced turbulence coefficient (k-ε model)
d_B	bulk bubble diameter (m)
$d_\perp$	bubble diameter perpendicular to main motion (m)
d	column diameter / width (m)
Eo	Eötvös Number
F_D	drag force (N m^{-3})
F_L	lift force (N m^{-3})
F_{TD}	turbulent dispersion force (N m^{-3})
F_{VM}	virtual mass force (N m^{-3})
F_W	wall force (N m^{-3})
g	acceleration of gravity (m s^{-2})
k	turbulent kinetic energy (m^2 s^{-2})
Mo	Morton Number
p	Pressure (Pa)
Re	Reynolds number
t	Time (s)
$\boldsymbol{v}$	velocity (m s^{-1})
x	coordinate along column width (m)
y	coordinate along column height (m)
z	coordinate along column depth (m)
α	volume fraction
ε	turbulent dissipation rate (m^2 s^{-3})

μ	dynamic viscosity (kg m^{-1} s^{-1})
ν	kinematic viscosity (m^2 s^{-1})
ρ	Density (kg m^{-3})
σ	surface tension (N m^{-1})

REFERENCES

[1] R. F. Mudde, W. K. Harteveld and H. E. A. van den Akker, "Uniform Flow in bubble-Columns," *Ind. Eng. Chem. Res.*, vol. 48, p. 148–158, **2009**.

[2] Y. Liao, R. Rzehak, D. Lucas and E. Krepper, "Baseline closure model for dispersed bubbly flow: Bubble coalescence and breakup," *Chemical Engineering Science* , vol. 122, pp. 336-349, **2015**.

[3] T. Wang and J. Wang, "Numerical simulations of gas liquid mass transfer in bubble columns with a CFD PBM coupled model," *Chemical Engineering Science*, vol. 62, no. 24, pp. 7107-7118, **2007**.

[4] F. Risso, V. Roig, Z. Amoura, G. Riboux and A.-M. Billet, "Wake attenuation in large Reynolds number dispersed two-phase flows," *Phil. Trans. R. Soc. A*, vol. 366, p. 2177, **2008**.

[5] G. Riboux, F. Risso and D. Legendre, "Experimental characterization of the agitation generated by bubbles rising at high Reynolds number," *Journal of Fluid Mechanics*, vol. 643, p. 509, **2010**.

[6] Y. Sato, M. Sadatomi and K. Sekoguchi, "Momentum and heat transfer in two-phase bubble flow I: Theory," *Int. J. Multiphase Flow*, vol. 7, p. 167, **1981**.

[7] A. Serizawa and I. Kataoka, "Turbulence suppression in bubbly two-phase flow," *Nuclear Engineering and Design*, vol. 122, p. 1, **1990**.

[8] W. P. Jones and B. E. Launder, "The Predicition of Laminarization with a two-equation model of turbulence," *Int. J. Heat Mass Transfer*, vol. 15, pp. 301-334, **1972**.

[9] E. Krepper, D. Lucas and H.-M. Prasser, "On the modelling of bubbly flow in vertical pipes," *Nuclear Engineering and Design*, vol. 235, p. 597, **2005**.

[10] M. V. Tabib, A. Roy and J. Joshi, "CFD simulation of bubble column - An analysis of interphase forces and turbulence models," *Chemical Engineering Journal*, vol. 139, pp. 589-614, **2008**.

[11] E. Krepper, C. Morel, B. Niceno and P. Ruyer, "CFD modeling of adiabatic bubbly flow," *Multiphase Science and Technology*, vol. 23, p. 129–164, **2011**.

[12] T. Ziegenhein, R. Rzehak and D. Lucas, "Transient simulation for large scale flow in bubble columns," *Chemical Engineering Science* , vol. 122, no. 0, pp. 1-13, **2015**.

[13] R. Rzehak and E. Krepper, "CFD modeling of bubble-induced turbulence," *International Journal of Multiphase Flow*, vol. 55, p. 138–155, **2013a**.

[14] T. Ziegenhein, D. Lucas, R. Rzehak and E. Krepper, "Closure relations for CFD simulation of bubble columns," Jeju, Korea, May 26-31, **2013b**.

[15] R. Masood, C. Rauh and A. Delgado, "CFD simulation of bubble column flows: An explicit algebraic Reynolds stress model approach," *International Journal of Multiphase Flow*, vol. 66, no. 0, pp. 11-25, **2014**.

[16] T. Ma, D. Lucas, T. Ziegenhein, J. Fröhlich and N. Deen, "Scale-adaptive simulation of a square cross-sectional bubble column," *Chemical Engineering Science,* vol. 131, pp. 101-108, **2015**.

[17] A. Sokolichin and G. Eigenberger, "Gas-liquid flow in bubble columns and loop reactors: Part I. Detailed modelling and numerical simulation," *Chemical Engineering Science,* vol. 49, no. 24, Part 2, pp. 5735-5746, **1994**.

[18] S. Becker, A. Sokolichin and G. Eigenberger, "Gas-liquid flow in bubble columns and loop reactors: Part II. Comparison of detailed experiments and flow simulations," *Chemical Engineering Science,* vol. 49, no. 24, Part 2, pp. 5747-5762, **1994**.

[19] D. Pfleger, S. Gomes, N. Gilbert and H.-G. Wagner, "Hydrodynamic simulations of laboratory scale bubble columns fundamental studies of the Eulerian-Eulerian modelling approach," *Chemical Engineering Science,* vol. 54, no. 21, pp. 5091-5099, **1999**.

[20] N. Deen, T. Solberg and B. Hjertager, "Large eddy simulation of the Gas-Liquid flow in a square cross-sectioned bubble column," *Chemical Engineering Science,* vol. 56, pp. 6341-6349, **2001**.

[21] A. Sokolichin, G. Eigenberger and A. Lapin, "Simulation of Buoyancy Driven Bubbly Flow: Established Simplifications and Open Questions," *Fluid Mechanics and Transport Phenomena,* vol. 50, pp. 24-45, **2004**.

[22] M. Diaz, F. Montes and M. Galan, "Influence of the lift force closures on the numerical simulation of bubble plumes in a rectangular bubble column," *Chemical Engineering Science,* vol. 64, pp. 930-944, **2009**.

[23] S. Ojima, K. Hayashi, S. Hosokawa and A. Tomiyama, "Distributions of void fraction and liquid velocity in air–water bubble column," *International Journal of Multiphase Flow,* vol. 67, pp. 111-121, **2014**.

[24] R. Rzehak and E. Krepper, "Closure models for turbulent bubbly flows: A CFD study," *Nuclear Engineering and Design,* vol. 265, pp. 701-711, **2013b**.

[25] D. Lucas, E. Krepper, H.-M. Prasser and A. Manera, "Stability effect of the lateral lift force in bubbly flows," Leipzig, Germany, **2007b**.

[26] J. E. Julia, L. Hernandez, S. Chiva and A. Vela, "Hydrodynamic characterization of a needle sparger rectangular bubble column: Homogeneous flow, static bubble plume and oscillating bubble plume," *Chemical Engineering Science,* vol. 62, no. 22, pp. 6361-6377, **2007**.

[27] M. Ishii and T. Hibiki, THERMO-FLUID DYNAMICS OF TWO-PHASE FLOW, 2nd ed., New York: Springer Science+Business Media, Inc., **2006**.

[28] H. A. Jakobsen, H. Lindborg and C. A. Dorao, "Modeling of bubble-Column Reactors: Progress and Limitations," *Ind. Eng. Chem. Res.,* vol. 44, p. 5107, **2005**.

[29] R. Rzehak and E. Krepper, "Bubbly flows with fixed polydispersity: Validation of a baseline closure model," *Nuclear Engineering and Design,* vol. 287, pp. 108-118, **2015**.

[30] R. Rzehak and S. Kriebitzsch, "Multiphase CFD-simulation of Bubbly Pipe Flow: A Code Comparison," *Int J Multiphase Flow*, **2014**.

[31] R. Rzehak, E. Krepper, Y. Liao, T. Ziegenhein, S. Kriebitzsch and D. Lucas, "Baseline Model for the Simulation of Bubbly Flows," *Chemical Engineering & Technology*, pp. 1972-1978, **2015**.

[32] T. Ziegenhein, R. Rzehak, E. Krepper and D. Lucas, "Numerical Simulation of Polydispersed Flow in bubble-Columns with the Inhomogeneous Multi-Size-Group Model," *Chemie Ingenieur Technik*, vol. 85, no. 7, pp. 1080-1091, **2013a**.

[33] C. Morel, "Turbulence modeling and first numerical simulations in turbulent two-phase flows," 11th Symposium on Turbulent Shear Flows, Grenoble, France, **1997**.

[34] A. A. Troshko and Y. A. Hassan, "A two-equation turbulence model of turbulent bubbly flows," *International Journal of Multiphase Flow*, vol. 27, p. 1965, **2001**.

[35] M. Politano, P. Carrica and J. Converti, "A model for turbulent polydisperse two-phase flow in vertical channels," *International Journal of Multiphase Flow*, vol. 29, p. 1153, **2003**.

[36] P. Spalart, "Strategies for turbulence modelling and simulations," *International Journal of Heat and Fluid Flow*, vol. 21, no. 3, pp. 252-263, **2000**.

[37] M. Ishii and N. Zuber, "Drag Coefficient and Relative Velocity in Bubbly, Droplet or Particulate Flows," *AlChE Journal*, vol. 25, p. 843, **1979**.

[38] A. Tomiyama, I. Kataoka, I. Zun and T. Sakaguchi, "Drag Coefficients of Single Bubbles under Normal and Micro Gravity Conditions," *JSME International Journal B*, vol. 41, p. 472, **1998**.

[39] I. Zun, "The transverse migration of bubbles influenced by walls in vertical bubbly flow," *International Journal of Multiphase Flow*, vol. 6, p. 583, **1980**.

[40] A. Tomiyama, "Single Bubbles in Stagnant Liquids and in Linear Shear Flows," Dresden, Germany, **2002**.

[41] D. Bothe, M. Schmidtke and H.-J. Warnecke, "VOF-Simulation of the Lift Force for Single Bubbles in a Simple Shear Flow," *Chem. Eng. Technol.*, vol. 29, p. 1048, **2006**.

[42] R. M. Wellek, A. K. Agrawal and A. H. P. Skelland, "Shape of Liquid Drops Moving in Liquid Media," *AlChE Journal*, vol. 12, p. 854, **1966**.

[43] D. Lucas and A. Tomiyama, "On the role of the lateral lift force in poly-dispersed bubbly flows," *International Journal of Multiphase Flow*, vol. 37, p. 1178, **2011**.

[44] A. Tomiyama, A. Sou, I. Zun, N. Kanami and T. Sakaguchi, "Effects of Eötvös number and dimensionless liquid volumetric flux on lateral motion of a bubble in a laminar duct flow," in *Advances in multiphase flow*, Amsterdam, **1995**.

[45] S. Hosokawa, A. Tomiyama, S. Misaki and T. Hamada, "Lateral Migration of Single Bubbles Due to the Presence of Wall," in *(FEDSM2002)*,, Montreal, Quebec, Canada, **2002**.

[46] R. Rzehak, E. Krepper and C. Lifante, "Comparative study of wall-force models for the simulation of bubbly flows," *Nuclear Engineering and Design,* vol. 253, pp. 41-49, **2012**.

[47] A. Burns, T. Frank, I. Hamill and J.-M. Shi, "The Favre Averaged Drag Model for Turbulent Dispersion in Eulerian Multi-Phase Flows," in *Paper No. 392*, Yokohama, Japan, **2004**.

[48] G. Mougin and J. Magnaudet, "The generalized Kirchhoff equations and their application to the interaction between a rigid body and an arbitrary time-dependent viscous flow," *International Journal of Multiphase Flow,* vol. 28, p. 1837, **2002**.

[49] Ansys, *CFX 14.5 Manual: CFX-Solver Modeling Guide.*, Canonsburg, Pennsylvania: Ansys, Inc., **2013**.

[50] D. Lucas, H.-M. Prasser and A. Manera, "Influence of the lift force on the stability of a bubble column," *Chemical Engineering Science,* vol. 60, p. 3609 – 3619, **2005**.

[51] M. H. bin Mohd Akbar , K. Hayashi , S. Hosokawa and A. Tomiyama, "Bubble tracking simulation of bubble-induced pseudoturbulence," *Multiphase Science and Technology,* vol. 24, no. 3, pp. 197-222, **2012**.

[52] M. L. de Bertodano, S.-J. Lee, J. R. T. Lahey and D. A. Drew, "The Prediction of Two-Phase Turbulence and Phase Distribution Phenomena Using a Reynolds Stress Model," *J. Fluids Eng.,* vol. 112, p. 107, **1990**.

[53] M. Lance, J. Mariè and J. Bataille, "Homogeneous turbulence in bubbly flows," *Journal of Fluids Engineering,* vol. 113, p. 295, **1991**.